

RECEIVED: March 30, 2018

ACCEPTED: May 13, 2018

PUBLISHED: May 25, 2018

Measurement of the CP asymmetry in $B^- \rightarrow D_s^- D^0$ and $B^- \rightarrow D^- D^0$ decays



The LHCb collaboration

E-mail: alison.tully@cern.ch

ABSTRACT: The CP asymmetry in $B^- \rightarrow D_s^- D^0$ and $B^- \rightarrow D^- D^0$ decays is measured using LHCb data corresponding to an integrated luminosity of 3.0 fb^{-1} , collected in pp collisions at centre-of-mass energies of 7 and 8 TeV. The results are $\mathcal{A}^{CP}(B^- \rightarrow D_s^- D^0) = (-0.4 \pm 0.5 \pm 0.5)\%$ and $\mathcal{A}^{CP}(B^- \rightarrow D^- D^0) = (2.3 \pm 2.7 \pm 0.4)\%$, where the first uncertainties are statistical and the second systematic. This is the first measurement of $\mathcal{A}^{CP}(B^- \rightarrow D_s^- D^0)$ and the most precise determination of $\mathcal{A}^{CP}(B^- \rightarrow D^- D^0)$. Neither result shows evidence of CP violation.

KEYWORDS: B physics, CP violation, Flavor physics, Hadron-Hadron scattering (experiments)

ARXIV EPRINT: [1803.10990](https://arxiv.org/abs/1803.10990)

Contents

1	Introduction	1
2	Detector and simulation	3
3	Candidate selection	4
4	Measurement of the raw asymmetries	5
5	Production and detection asymmetries	7
6	Results and conclusions	8
	The LHCb collaboration	12

1 Introduction

Weak decays of heavy hadrons are governed by transition amplitudes that are proportional to the elements $V_{qq'}$ of the unitary 3×3 Cabibbo-Kobayashi-Maskawa (CKM) matrix [1, 2], a crucial component of the Standard Model (SM) of elementary particle physics. Different decay rates between heavy-flavoured hadrons and their antiparticles are possible if there is interference between two or more quark-level transitions with different phases. The corresponding violation of CP symmetry was first observed in neutral kaon decays [3]. In B decays, CP violation was first observed in the interference between a decay with and without mixing [4, 5] and later also directly in the decays of B^0 mesons [6, 7].

The decays of charged or neutral B mesons to two charm mesons are driven by tree-level and loop-level amplitudes, as illustrated in figure 1. Annihilation diagrams also contribute, but to a lesser extent. The decays $\bar{B}^0 \rightarrow D^+ D^-$, $\bar{B}^0 \rightarrow D^0 \bar{D}^0$ and $B^- \rightarrow D^- D^0$ are related by isospin symmetry,¹ and expressions that relate the branching fractions and CP asymmetries, as well as nonfactorizable effects, have been derived [8, 9].

The CP asymmetry in the decay of the B^- meson to two charm mesons is defined as

$$\mathcal{A}^{CP}(B^- \rightarrow D_{(s)}^- D^0) \equiv \frac{\Gamma(B^- \rightarrow D_{(s)}^- D^0) - \Gamma(B^+ \rightarrow D_{(s)}^+ \bar{D}^0)}{\Gamma(B^- \rightarrow D_{(s)}^- D^0) + \Gamma(B^+ \rightarrow D_{(s)}^+ \bar{D}^0)}. \quad (1.1)$$

Nonzero CP asymmetries in $B^- \rightarrow D_{(s)}^- D^0$ decays are expected [10–13] due to interference of contributions from tree-level amplitudes with those from loop-level and annihilation amplitudes. In the SM, these CP asymmetries are expected to be small, $\mathcal{O}(10^{-2})$. New physics contributions can enhance the CP asymmetry in these decays [12–15]. The most

¹Unless specified otherwise, charge conjugation is implied throughout the paper.

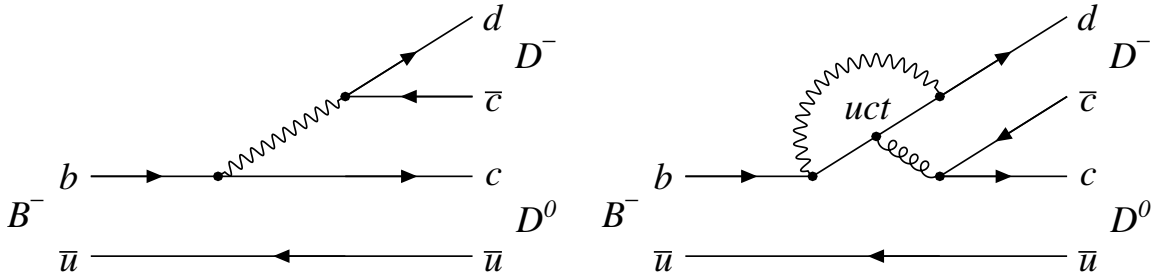


Figure 1. Illustration of (left) tree diagram and (right) loop diagram contributions to the decay $B^- \rightarrow D^- D^0$. Similar diagrams, with the d replaced by s , apply to the decay $B^- \rightarrow D_s^- D^0$.

precise measurements of the CP asymmetry in $B^- \rightarrow D^- D^0$ decays are from the Belle and BaBar experiments, $\mathcal{A}^{CP} = (0 \pm 8 \pm 2)\%$ [16] and $\mathcal{A}^{CP} = (-13 \pm 14 \pm 2)\%$ [17], respectively, where the first uncertainties are statistical and the second systematic. The CP asymmetry in $B^- \rightarrow D_s^- D^0$ decays has not been measured before.

This paper describes a measurement of the CP asymmetry in $B^- \rightarrow D_s^- D^0$ and $B^- \rightarrow D^- D^0$ decays, using pp collision data corresponding to an integrated luminosity of 3.0 fb^{-1} , of which 1.0 fb^{-1} was taken in 2011 at a centre-of-mass energy of $\sqrt{s} = 7 \text{ TeV}$ and 2.0 fb^{-1} in 2012 at $\sqrt{s} = 8 \text{ TeV}$. Charm mesons are reconstructed in the following decays: $D^0 \rightarrow K^- \pi^+$, $D^0 \rightarrow K^- \pi^+ \pi^- \pi^+$, $D^- \rightarrow K^+ \pi^- \pi^-$, and $D_s^- \rightarrow K^- K^+ \pi^-$.

The determinations of $\mathcal{A}^{CP}(B^- \rightarrow D_{(s)}^- D^0)$ are based on the measurements of the raw asymmetries

$$A_{\text{raw}} \equiv \frac{N(B^- \rightarrow D_{(s)}^- D^0) - N(B^+ \rightarrow D_{(s)}^+ \bar{D}^0)}{N(B^- \rightarrow D_{(s)}^- D^0) + N(B^+ \rightarrow D_{(s)}^+ \bar{D}^0)}, \quad (1.2)$$

where N indicates the observed yield in the respective decay channel. The raw asymmetries include the asymmetry in B production and detection efficiencies of the final states. If the asymmetries are small, higher-order terms corresponding to products of the asymmetries can be neglected, and the following relation holds

$$\mathcal{A}^{CP} = A_{\text{raw}} - A_P - A_D, \quad (1.3)$$

where A_P is the asymmetry in the production cross-sections, σ , of B^\pm mesons,

$$A_P \equiv \frac{\sigma(B^-) - \sigma(B^+)}{\sigma(B^-) + \sigma(B^+)}, \quad (1.4)$$

and A_D is the asymmetry of the detection efficiencies, ε ,

$$A_D \equiv \frac{\varepsilon(B^- \rightarrow D_{(s)}^- D^0) - \varepsilon(B^+ \rightarrow D_{(s)}^+ \bar{D}^0)}{\varepsilon(B^- \rightarrow D_{(s)}^- D^0) + \varepsilon(B^+ \rightarrow D_{(s)}^+ \bar{D}^0)}. \quad (1.5)$$

2 Detector and simulation

The LHCb detector [18, 19] is a single-arm forward spectrometer covering the pseudo-rapidity range $2 < \eta < 5$, designed for the study of particles containing b or c quarks. The detector includes a high-precision tracking system consisting of a silicon-strip vertex detector surrounding the pp interaction region [20], a large-area silicon-strip detector located upstream of a dipole magnet with a bending power of about 4 Tm, and three stations of silicon-strip detectors and straw drift tubes [21] placed downstream of the magnet. The polarity of the dipole magnet is reversed periodically throughout data-taking, to cancel, to first order, asymmetries in the detection efficiency due to nonuniformities in the detector response. The configuration with the magnetic field vertically upwards (downwards) bends positively (negatively) charged particles in the horizontal plane towards the centre of the LHC.

The tracking system provides a measurement of momentum, p , of charged particles with a relative uncertainty that varies from 0.5% at low momentum to 1.0% at $200\,\text{GeV}/c$. The minimum distance of a track to a primary vertex (PV), the impact parameter (IP), is measured with a resolution of $(15 + 29/p_T)\,\mu\text{m}$, where p_T is the component of the momentum transverse to the beam, in GeV/c . Different types of charged hadrons are distinguished using information from two ring-imaging Cherenkov (RICH) detectors [22]. Photons, electrons and hadrons are identified by a calorimeter system consisting of scintillating-pad and preshower detectors, an electromagnetic calorimeter and a hadronic calorimeter. Muons are identified by a system composed of alternating layers of iron and multiwire proportional chambers [23].

The online event selection is performed by a trigger [24], which consists of a hardware stage, based on information from the calorimeter and muon systems, followed by a software stage, which applies a full event reconstruction. At the hardware trigger stage, events are required to have a muon with high p_T or a hadron, photon or electron with high transverse energy in the calorimeters. The software trigger requires a two-, three- or four-track secondary vertex with a large sum of the transverse momenta of the tracks and a significant displacement from the primary pp interaction vertices. At least one track should have $p_T > 1.7\,\text{GeV}/c$ and χ^2_{IP} with respect to any PV greater than 16, where χ^2_{IP} is defined as the difference in fit χ^2 of a given PV reconstructed with and without the considered particle. A multivariate algorithm [25] is used for the identification of secondary vertices consistent with the decay of a b hadron.

Simulated events are used for the training of a multivariate selection, and for determining the shape of the invariant-mass distributions of the signals. In the simulation, pp collisions with $B^- \rightarrow D_{(s)}^- D^0$ decays are generated using PYTHIA [26, 27] with a specific LHCb configuration [28]. Decays of hadronic particles are described by EVTGEN [29], in which final-state radiation is generated using PHOTOS [30]. The interaction of the generated particles with the detector, and its response, are implemented using the GEANT4 toolkit [31, 32] as described in ref. [33]. Known discrepancies in the simulation for the mass scale, the momentum resolution and the RICH response are corrected using data-driven methods.

3 Candidate selection

The offline selection of $B^- \rightarrow D_{(s)}^- D^0$ candidates is a two-step process. First, loose criteria are applied to select candidates compatible with the decay $B^- \rightarrow D_{(s)}^- D^0$. Second, a multivariate selection is applied and optimized by minimizing the statistical uncertainty on the asymmetry measurement.

Charm meson candidates are constructed by combining 2, 3 or 4 final-state tracks that are incompatible with originating from any reconstructed primary vertex ($\chi^2_{\text{IP}} > 4$). In addition, the sum of the transverse momenta of the tracks must exceed $1.8 \text{ GeV}/c$, the invariant mass must be within $\pm 25 \text{ MeV}/c^2$ of the known charm meson mass [34] and the tracks are required to form a vertex with good fit χ^2 . Particle identification (PID) criteria are also applied to the final-state particles, such that particles that have a significantly larger likelihood to be a kaon than a pion are not used as a pion candidate, and conversely. Three-track combinations that are compatible with both $D^- \rightarrow K^+ \pi^- \pi^-$ and $D_s^- \rightarrow K^- K^+ \pi^-$ decays are categorized as either D^- or D_s^- , based on the invariant mass of the three-track combination, the compatibility of opposite-charge track combinations with the $\phi \rightarrow K^+ K^-$ decay, and the PID information of the final-state tracks [35].

In events with at least one D^- or D_s^- candidate and at least one D^0 candidate, the charm mesons are combined to form a B^- candidate if their invariant mass is in the range $4.8 - 7.0 \text{ GeV}/c^2$. The B^- candidate is required to form a vertex with good fit χ^2 , and have a transverse momentum in excess of $4.0 \text{ GeV}/c$. The resulting trajectory of the B^- candidate must be consistent with originating from the associated PV, which is the PV for which the B^- candidate has the smallest value of χ^2_{IP} . The reconstructed decay time divided by its uncertainty, $\tau/\Delta\tau$, of D^0 and D_s^- mesons with respect to the B^- vertex is required to exceed -3 , while for the longer-lived D^- meson it is required to exceed $+3$. The tighter decay-time significance requirement on the D^- eliminates background from $B^- \rightarrow D^0 \pi^- \pi^+ \pi^-$ decays where the negatively charged pion is misidentified as a kaon. In the offline selection, trigger signals are associated with reconstructed particles. Signal candidates are selected if the trigger decision was due to the candidate itself, hereafter called trigger on signal (TOS), or due to the other particles produced in the pp collision, hereafter called trigger independent of signal (TIS).

The invariant-mass resolution of $B^- \rightarrow D_{(s)}^- D^0$ decays is significantly improved by performing a constrained fit [36]. In this fit, the decay products from each vertex are constrained to originate from a common vertex, the B^- vertex is constrained to originate from the associated PV, and the invariant masses of the D^0 and the $D_{(s)}^-$ mesons are constrained to their known masses [34],

To reduce the combinatorial background, while keeping the signal efficiency as large as possible, a multivariate selection based on a boosted decision tree (BDT) [37, 38] is applied. The following variables are used as input to the BDT: the transverse momentum and the ratio between the likelihoods of the kaon and pion hypotheses of each final-state track; the fit χ^2 of the B^- candidate and of both charm meson vertices; the value of χ^2_{IP} of the B^- candidate; the values of $\tau/\Delta\tau$ for the B^- and for both charm meson candidates; the invariant masses of the reconstructed charm meson candidates; and the invariant masses

of opposite-charge tracks from the $D_{(s)}^-$ candidate. Separate trainings are performed for the $B^- \rightarrow D_s^- D^0$ and the $B^- \rightarrow D^- D^0$ modes, and for both D^0 decay channels. The BDT is trained using simulated B^- signal samples and candidates in the upper mass sideband of the B^- meson ($5350 < m(D_{(s)}^- D^0) < 6200 \text{ MeV}/c^2$) as background. To increase the size of the background sample for the BDT training, the charm meson invariant-mass intervals are increased from $\pm 25 \text{ MeV}/c^2$ to $\pm 75 \text{ MeV}/c^2$, and ‘wrong-sign’ $B^- \rightarrow D_{(s)}^- \bar{D}^0$ candidates are also included. Checks have been performed to verify that for all the variables used in the BDT the simulated B^- decays describe the observed signals in data well, and that selections on the BDT output do not alter the shape of the invariant-mass distribution of the combinatorial background.

The BDT combines all input variables into a single discriminant. The optimal requirement on this value is determined by maximizing $N_S/\sqrt{N_S + N_B}$, where N_S is the expected signal yield, determined from the initial signal yield in data multiplied by the BDT efficiency from simulation, and N_B is the background yield extrapolated from the upper mass sideband to a $\pm 20 \text{ MeV}/c^2$ interval around the B^- mass. This selection has an efficiency of 98% (90%) for $B^- \rightarrow D_s^- D^0$ ($D^- D^0$) decays, and a background rejection of 88% (93%).

4 Measurement of the raw asymmetries

After the event selection, the signal yields and the raw asymmetries are determined by fitting a model of the invariant-mass distribution of $B^- \rightarrow D_{(s)}^- D^0$ candidates to the data. The model includes components for the signal decays, a background from $B^- \rightarrow K^- K^+ \pi^- D^0$ decays and a combinatorial background.

The invariant-mass distribution of $B^- \rightarrow D_{(s)}^- D^0$ decays is described by a sum of two Crystal Ball (CB) [39] functions, with power-law tails proportional to $[m(D_{(s)}^- D^0) - m(B^-)]^{-2}$ in opposite directions, and with a common peak position. The tail parameters of the CB functions, as well as the ratio of the widths of both CB components, are obtained from simulation. The peak position of the B^- signal and the width of one of the CB functions are free parameters in the fits to the data. This model provides a good description of the $B^- \rightarrow D_{(s)}^- D^0$ signals.

The Cabibbo-favoured $B^- \rightarrow K^- K^+ \pi^- D^0$ decay is a background to the $B^- \rightarrow D_s^- D^0$ channel, despite being strongly suppressed by the invariant-mass requirement on the $K^- K^+ \pi^-$ mass. This background is modelled by a single Gaussian function, whose width is determined from a fit to simulated decays and the yields determined from the D_s^- sidebands. The yield of this background is about 30 times smaller than that of the signal, and the shape of the invariant-mass distribution is twice as wide. The combinatorial background is described by an exponential function. Candidates originating from partially reconstructed $B^- \rightarrow D_{(s)}^{*-} D^0$ and $B^- \rightarrow D_{(s)}^- D^{*0}$ decays do not contribute to the background since their reconstructed invariant mass is below the lower limit of the fit region.

Separate unbinned extended maximum likelihood fits are used to describe the invariant-mass distributions of candidates with $D^0 \rightarrow K^- \pi^+$ decays and those with $D^0 \rightarrow K^- \pi^+ \pi^- \pi^+$ decays. Figure 2 shows the fits to the invariant-mass distributions in the fit region,

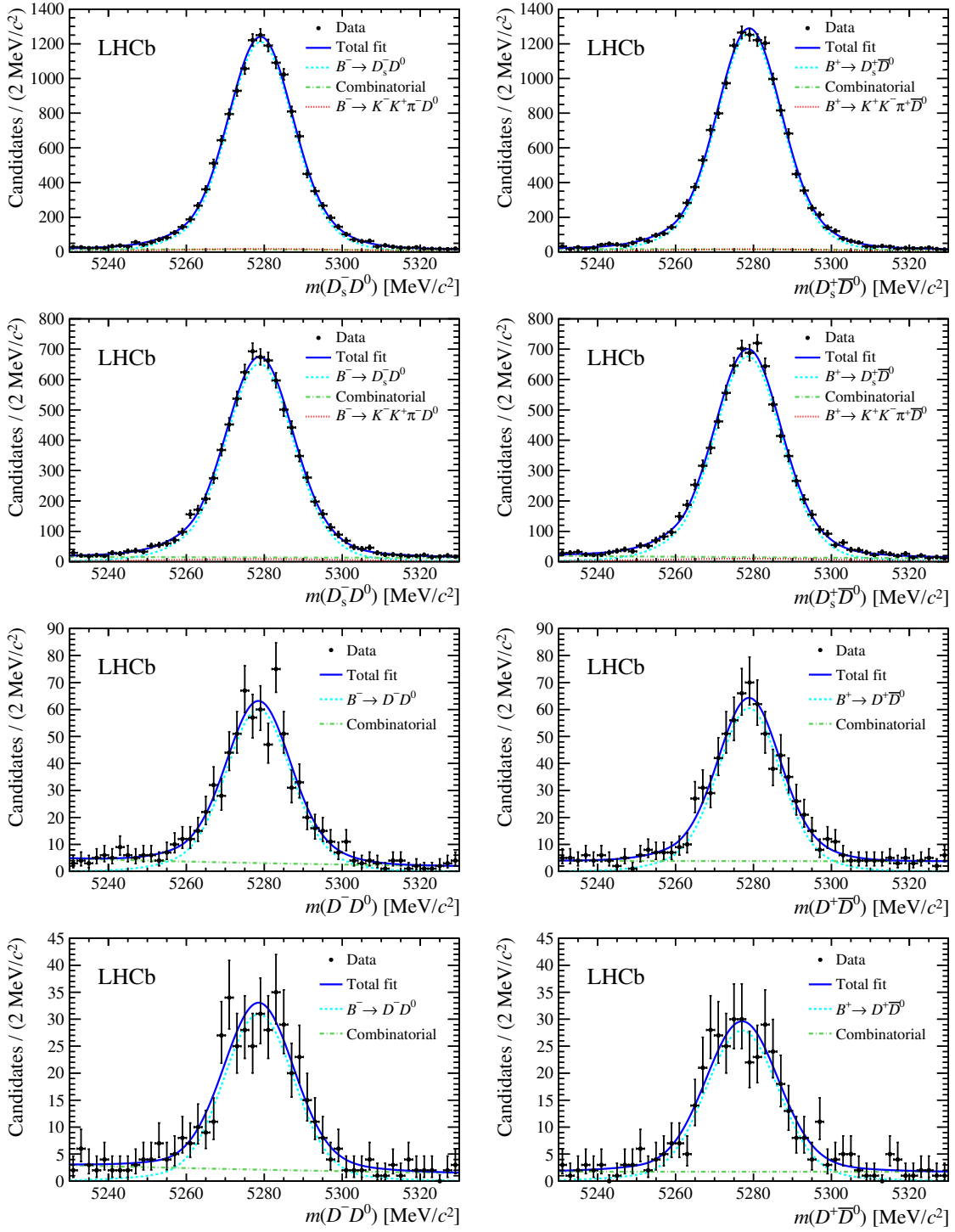


Figure 2. Invariant-mass distribution of $B^- \rightarrow D_{(s)}^- D^0$ candidates, separated by charge. The top row plots are $B^- \rightarrow D_s^- D^0$ decays with $D^0 \rightarrow K^- \pi^+$, the second row with $D^0 \rightarrow K^- \pi^+ \pi^- \pi^+$. The plots in the third row correspond to $B^- \rightarrow D^- D^0$ candidates with $D^0 \rightarrow K^- \pi^+$, the bottom row with $D^0 \rightarrow K^- \pi^+ \pi^- \pi^+$. The left plots are B^- candidates, the right plots B^+ candidates. The overlaid curves show the fits described in the text.

Channel	$N(B^-)$	$N(B^+)$	A_{raw}
$B^- \rightarrow D_s^- D^0$, $D^0 \rightarrow K^- \pi^+$	13659 ± 129	14209 ± 132	$(-2.0 \pm 0.7)\%$
$B^- \rightarrow D_s^- D^0$, $D^0 \rightarrow K^- \pi^+ \pi^- \pi^+$	7717 ± 103	7945 ± 104	$(-1.5 \pm 0.9)\%$
$B^- \rightarrow D_s^- D^0$, combined	21375 ± 165	22153 ± 168	$(-1.8 \pm 0.5)\%$
$B^- \rightarrow D^- D^0$, $D^0 \rightarrow K^- \pi^+$	678 ± 32	660 ± 31	$(-1.3 \pm 3.3)\%$
$B^- \rightarrow D^- D^0$, $D^0 \rightarrow K^- \pi^+ \pi^- \pi^+$	369 ± 24	345 ± 24	$(-3.4 \pm 4.7)\%$
$B^- \rightarrow D^- D^0$, combined	1047 ± 40	1005 ± 39	$(-2.0 \pm 2.7)\%$

Table 1. Yields and raw asymmetries for $B^- \rightarrow D_{(s)}^- D^0$ decays.

$5230 < m(D_{(s)}^- D^0) < 5330 \text{ MeV}/c^2$, of the $B^- \rightarrow D_s^- D^0$ and $B^- \rightarrow D^- D^0$ channels, separated by charge and decay mode. The signal yields and corresponding raw asymmetries, calculated according to eq. (1.2), are listed in table 1. No significant dependence on the magnet polarity or data taking year is observed. Inaccuracies in the modelling of the signal or background may result in a small biases of the yields, but are not expected to introduce additional asymmetries, therefore no systematic uncertainties are attributed to the modelling of the signal and background shapes.

5 Production and detection asymmetries

The production asymmetry between B^- and B^+ mesons at LHCb has been measured to be $A_P = (-0.5 \pm 0.4)\%$ using the $B^- \rightarrow D^0 \pi^-$ decay [40], and no significant dependence of A_P on the transverse momentum or on the rapidity of the B meson has been observed.

Four contributions to the asymmetry of the detection efficiencies are considered: asymmetries in the tracking efficiency, the different K^\pm interaction cross-sections with the detector material, and the trigger and particle identification efficiencies.

The momentum-dependent tracking efficiency for pions has been determined by comparing the yields of fully to partially reconstructed $D^{*+} \rightarrow (D^0 \rightarrow K^- \pi^+ \pi^- \pi^+) \pi^+$ decays [41]. The corresponding asymmetries are summed for all final-state tracks of simulated $B^- \rightarrow D_{(s)}^- D^0$ events. After averaging over data-taking year and magnet polarity, the tracking asymmetry is determined to be $(0.18 \pm 0.07)\%$ for $B^- \rightarrow D_s^- D^0$ and $(0.21 \pm 0.07)\%$ for $B^- \rightarrow D^- D^0$ decays, where the uncertainties are due to the finite sample of D^{*+} decays used for the tracking efficiency measurement.

The interaction cross-section of K^- mesons with matter is significantly larger than that of K^+ mesons, resulting in a large asymmetry of the charged kaon detection efficiency. The momentum-dependent difference in the detection asymmetry between kaons and pions has been measured by comparing the yield of $D^+ \rightarrow K^- \pi^+ \pi^+$ to the yield of $D^+ \rightarrow K_s^0 \pi^+$ decays [42]. These asymmetries, convoluted with the momentum spectra of the final-state kaons, result in a contribution to the detection asymmetry of $(-1.04 \pm 0.16)\%$ for $B^- \rightarrow D_s^- D^0$ decays, where the uncertainty is due to the finite samples of D^+ decays. For

$B^- \rightarrow D^- D^0$ decays, this asymmetry cancels to first order since it has one K^+ and one K^- particle in the final state, and the resulting asymmetry is $(0.02 \pm 0.01)\%$.

The charge asymmetry of TIS candidates is independent of the signal decay channel in consideration and has been measured in $\bar{B} \rightarrow D^0 \mu^- \bar{\nu}_\mu X$ decays [40]. After weighting by the TIS fraction, the asymmetry is found to be 0.04% and is neglected. A nonuniform response of the calorimeter may result in a charge asymmetry of the TOS signal. Large samples of $D^0 \rightarrow K^- \pi^+$ decays have been used to determine the p_T -dependent trigger efficiencies and corresponding charge asymmetries for both pions and kaons. After convoluting these efficiencies with the simulated p_T spectra, averaging by data-taking year and magnet polarity, and multiplying by the TOS fraction of the signal, the resulting asymmetry is below 0.05%, and is considered to be negligible.

In the candidate selection, particle identification criteria that rely on information from the RICH detectors are used. Possible charge asymmetries in the efficiencies of these selections are studied with samples of $D^0 \rightarrow K^- \pi^+$ that were selected without PID requirements. Depending on assumptions on the correlation between the PID and other variables in the multivariate selection, asymmetries smaller than 0.1% are found. Therefore, no correction is applied, and a 0.1% uncertainty is assigned.

The uncertainties of the contributions to the production and detection asymmetry are considered to be uncorrelated and result in a value of $A_P + A_D$ of $(-1.4 \pm 0.5)\%$ for $B^- \rightarrow D_s^- D^0$ and $(-0.3 \pm 0.4)\%$ for $B^- \rightarrow D^- D^0$ decays. Changes in the fit model have a negligible effect on the measured asymmetry.

6 Results and conclusions

The CP asymmetries are determined by subtracting the production and detection asymmetries from the measured raw asymmetry according to eq. (1.3). The obtained results are

$$\begin{aligned}\mathcal{A}^{CP}(B^- \rightarrow D_s^- D^0) &= (-0.4 \pm 0.5 \pm 0.5)\%, \\ \mathcal{A}^{CP}(B^- \rightarrow D^- D^0) &= (-2.3 \pm 2.7 \pm 0.4)\%,\end{aligned}$$

where the first uncertainties are statistical and the second systematic. The measured value of $\mathcal{A}^{CP}(B^- \rightarrow D_s^- D^0)$ provides constraints on the range of CP violation predicted for a new physics model with R -parity violating supersymmetry [13].

In conclusion, the CP asymmetry in $B^- \rightarrow D_s^- D^0$ decays has been measured for the first time and the uncertainty on the CP asymmetry in $B^- \rightarrow D^- D^0$ decays has been reduced by more than a factor two with respect to previous measurements. No evidence for CP violation in $B^- \rightarrow D_{(s)}^- D^0$ decays has been found.

Acknowledgments

We express our gratitude to our colleagues in the CERN accelerator departments for the excellent performance of the LHC. We thank the technical and administrative staff at the LHCb institutes. We acknowledge support from CERN and from the national agencies: CAPES, CNPq, FAPERJ and FINEP (Brazil); MOST and NSFC (China);

CNRS/IN2P3 (France); BMBF, DFG and MPG (Germany); INFN (Italy); NWO (The Netherlands); MNiSW and NCN (Poland); MEN/IFA (Romania); MinES and FASO (Russia); MinECo (Spain); SNSF and SER (Switzerland); NASU (Ukraine); STFC (United Kingdom); NSF (U.S.A.). We acknowledge the computing resources that are provided by CERN, IN2P3 (France), KIT and DESY (Germany), INFN (Italy), SURF (The Netherlands), PIC (Spain), GridPP (United Kingdom), RRCKI and Yandex LLC (Russia), CSCS (Switzerland), IFIN-HH (Romania), CBPF (Brazil), PL-GRID (Poland) and OSC (U.S.A.). We are indebted to the communities behind the multiple open-source software packages on which we depend. Individual groups or members have received support from AvH Foundation (Germany), EPLANET, Marie Skłodowska-Curie Actions and ERC (European Union), ANR, Labex P2IO and OCEVU, and Région Auvergne-Rhône-Alpes (France), Key Research Program of Frontier Sciences of CAS, CAS PIFI, and the Thousand Talents Program (China), RFBR, RSF and Yandex LLC (Russia), GVA, XuntaGal and GENCAT (Spain), Herchel Smith Fund, the Royal Society, the English-Speaking Union and the Leverhulme Trust (United Kingdom).

Open Access. This article is distributed under the terms of the Creative Commons Attribution License ([CC-BY 4.0](#)), which permits any use, distribution and reproduction in any medium, provided the original author(s) and source are credited.

References

- [1] N. Cabibbo, *Unitary symmetry and leptonic decays*, *Phys. Rev. Lett.* **10** (1963) 531 [[INSPIRE](#)].
- [2] M. Kobayashi and T. Maskawa, *CP violation in the renormalizable theory of weak interaction*, *Prog. Theor. Phys.* **49** (1973) 652 [[INSPIRE](#)].
- [3] J.H. Christenson, J.W. Cronin, V.L. Fitch and R. Turlay, *Evidence for the 2π decay of the K_2^0 meson*, *Phys. Rev. Lett.* **13** (1964) 138 [[INSPIRE](#)].
- [4] BABAR collaboration, B. Aubert et al., *Observation of CP violation in the B^0 meson system*, *Phys. Rev. Lett.* **87** (2001) 091801 [[hep-ex/0107013](#)] [[INSPIRE](#)].
- [5] BELLE collaboration, K. Abe et al., *Observation of large CP violation in the neutral B meson system*, *Phys. Rev. Lett.* **87** (2001) 091802 [[hep-ex/0107061](#)] [[INSPIRE](#)].
- [6] BABAR collaboration, B. Aubert et al., *Direct CP-violation in $B^0 \rightarrow K^+ \pi^-$ decays*, *Phys. Rev. Lett.* **93** (2004) 131801 [[hep-ex/0407057](#)] [[INSPIRE](#)].
- [7] BELLE collaboration, Y. Chao et al., *Evidence for direct CP violation in $B^0 \rightarrow K^+ \pi^-$ decays*, *Phys. Rev. Lett.* **93** (2004) 191802 [[hep-ex/0408100](#)] [[INSPIRE](#)].
- [8] D. Sahoo, H.-Y. Cheng, C.-W. Chiang, C.S. Kim and R. Sinha, *Prediction of the CP asymmetry C_{00} in $B^0 \rightarrow D^0 \bar{D}^0$ decay*, *JHEP* **11** (2017) 087 [[arXiv:1709.08301](#)] [[INSPIRE](#)].
- [9] L. Bel, K. De Bruyn, R. Fleischer, M. Mulder and N. Tuning, *Anatomy of $B \rightarrow D \bar{D}$ decays*, *JHEP* **07** (2015) 108 [[arXiv:1505.01361](#)] [[INSPIRE](#)].
- [10] R.-H. Li, X.-X. Wang, A.I. Sanda and C.-D. Lu, *Decays of B meson to two charmed mesons*, *Phys. Rev. D* **81** (2010) 034006 [[arXiv:0910.1424](#)] [[INSPIRE](#)].
- [11] H.-F. Fu, G.-L. Wang, Z.-H. Wang and X.-J. Chen, *Semi-leptonic and non-leptonic B meson decays to charmed mesons*, *Chin. Phys. Lett.* **28** (2011) 121301 [[arXiv:1202.1221](#)] [[INSPIRE](#)].

- [12] L.-X. Lü, Z.-J. Xiao, S.-W. Wang and W.-J. Li, *Double charm decays of B mesons in the mSUGRA model*, *Commun. Theor. Phys.* **56** (2011) 125 [[arXiv:1008.4987](#)] [[INSPIRE](#)].
- [13] C.S. Kim, R.-M. Wang and Y.-D. Yang, *Studying double charm decays of $B_{u,d}$ and B_s mesons in the MSSM with R -parity violation*, *Phys. Rev. D* **79** (2009) 055004 [[arXiv:0812.4136](#)] [[INSPIRE](#)].
- [14] Y.-G. Xu and R.-M. Wang, *Studying the fourth generation quark contributions to the double charm decays $B_{(s)} \rightarrow D_{(s)}^{(*)} D_s^{(*)}$* , *Int. J. Theor. Phys.* **55** (2016) 5290 [[INSPIRE](#)].
- [15] M. Jung and S. Schacht, *Standard model predictions and new physics sensitivity in $B \rightarrow DD$ decays*, *Phys. Rev. D* **91** (2015) 034027 [[arXiv:1410.8396](#)] [[INSPIRE](#)].
- [16] BELLE collaboration, I. Adachi et al., *Measurement of the branching fraction and charge asymmetry of the decay $B^+ \rightarrow D^+ \bar{D}^0$ and search for $B^0 \rightarrow D^0 \bar{D}^0$* , *Phys. Rev. D* **77** (2008) 091101 [[arXiv:0802.2988](#)] [[INSPIRE](#)].
- [17] BABAR collaboration, B. Aubert et al., *Measurement of branching fractions and CP -violating charge asymmetries for B -meson decays to $D^{(*)} \bar{D}^{(*)}$, and implications for the CKM angle γ* , *Phys. Rev. D* **73** (2006) 112004 [[hep-ex/0604037](#)] [[INSPIRE](#)].
- [18] LHCb collaboration, *The LHCb detector at the LHC*, 2008 *JINST* **3** S08005 [[INSPIRE](#)].
- [19] LHCb collaboration, *LHCb detector performance*, *Int. J. Mod. Phys. A* **30** (2015) 1530022 [[arXiv:1412.6352](#)] [[INSPIRE](#)].
- [20] R. Aaij et al., *Performance of the LHCb Vertex Locator*, 2014 *JINST* **9** P09007 [[arXiv:1405.7808](#)] [[INSPIRE](#)].
- [21] R. Arink et al., *Performance of the LHCb Outer Tracker*, 2014 *JINST* **9** P01002 [[arXiv:1311.3893](#)] [[INSPIRE](#)].
- [22] M. Adinolfi et al., *Performance of the LHCb RICH detector at the LHC*, *Eur. Phys. J. C* **73** (2013) 2431 [[arXiv:1211.6759](#)] [[INSPIRE](#)].
- [23] A.A. Alves Jr. et al., *Performance of the LHCb muon system*, 2013 *JINST* **8** P02022 [[arXiv:1211.1346](#)] [[INSPIRE](#)].
- [24] R. Aaij et al., *The LHCb trigger and its performance in 2011*, 2013 *JINST* **8** P04022 [[arXiv:1211.3055](#)] [[INSPIRE](#)].
- [25] V.V. Gligorov and M. Williams, *Efficient, reliable and fast high-level triggering using a bonsai boosted decision tree*, 2013 *JINST* **8** P02013 [[arXiv:1210.6861](#)] [[INSPIRE](#)].
- [26] T. Sjöstrand, S. Mrenna and P.Z. Skands, *A brief introduction to PYTHIA 8.1*, *Comput. Phys. Commun.* **178** (2008) 852 [[arXiv:0710.3820](#)] [[INSPIRE](#)].
- [27] T. Sjöstrand, S. Mrenna and P.Z. Skands, *PYTHIA 6.4 physics and manual*, *JHEP* **05** (2006) 026 [[hep-ph/0603175](#)] [[INSPIRE](#)].
- [28] LHCb collaboration, *Handling of the generation of primary events in Gauss, the LHCb simulation framework*, *J. Phys. Conf. Ser.* **331** (2011) 032047 [[INSPIRE](#)].
- [29] D.J. Lange, *The EvtGen particle decay simulation package*, *Nucl. Instrum. Meth. A* **462** (2001) 152 [[INSPIRE](#)].
- [30] P. Golonka and Z. Was, *PHOTOS Monte Carlo: A precision tool for QED corrections in Z and W decays*, *Eur. Phys. J. C* **45** (2006) 97 [[hep-ph/0506026](#)] [[INSPIRE](#)].

- [31] GEANT4 collaboration, J. Allison et al., *Geant4 developments and applications*, *IEEE Trans. Nucl. Sci.* **53** (2006) 270 [[INSPIRE](#)].
- [32] GEANT4 collaboration, S. Agostinelli et al., *GEANT4: A simulation toolkit*, *Nucl. Instrum. Meth. A* **506** (2003) 250 [[INSPIRE](#)].
- [33] M. Clemencic et al., *The LHCb simulation application, Gauss: Design, evolution and experience*, *J. Phys. Conf. Ser.* **331** (2011) 032023 [[INSPIRE](#)].
- [34] PARTICLE DATA GROUP collaboration, C. Patrignani et al., *Review of particle physics*, *Chin. Phys. C* **40** (2016) 100001 [[INSPIRE](#)].
- [35] LHCb collaboration, *Study of beauty hadron decays into pairs of charm hadrons*, *Phys. Rev. Lett.* **112** (2014) 202001 [[arXiv:1403.3606](#)] [[INSPIRE](#)].
- [36] W.D. Hulsbergen, *Decay chain fitting with a Kalman filter*, *Nucl. Instrum. Meth. A* **552** (2005) 566 [[physics/0503191](#)] [[INSPIRE](#)].
- [37] L. Breiman, J.H. Friedman, R.A. Olshen and C.J. Stone, *Classification and regression trees*, Wadsworth International Group, Belmont, California, U.S.A. (1984).
- [38] B.P. Roe, H.-J. Yang, J. Zhu, Y. Liu, I. Stancu and G. McGregor, *Boosted decision trees, an alternative to artificial neural networks*, *Nucl. Instrum. Meth. A* **543** (2005) 577 [[physics/0408124](#)] [[INSPIRE](#)].
- [39] T. Skwarnicki, *A study of the radiative cascade transitions between the Upsilon-prime and Upsilon resonances*, Ph.D. Thesis, Institute of Nuclear Physics, Krakow (1986) [DESY-F31-86-02] [[INSPIRE](#)].
- [40] LHCb collaboration, *Measurement of the B^\pm production asymmetry and the CP asymmetry in $B^\pm \rightarrow J/\psi K^\pm$ decays*, *Phys. Rev. D* **95** (2017) 052005 [[arXiv:1701.05501](#)] [[INSPIRE](#)].
- [41] LHCb collaboration, *Measurement of the $D_s^+ - D_s^-$ production asymmetry in 7 TeV pp collisions*, *Phys. Lett. B* **713** (2012) 186 [[arXiv:1205.0897](#)] [[INSPIRE](#)].
- [42] LHCb collaboration, *Measurement of CP asymmetry in $D^0 \rightarrow K^- K^+$ and $D^0 \rightarrow \pi^- \pi^+$ decays*, *JHEP* **07** (2014) 041 [[arXiv:1405.2797](#)] [[INSPIRE](#)].

The LHCb collaboration

R. Aaij⁴³, B. Adeva³⁹, M. Adinolfi⁴⁸, Z. Ajaltouni⁵, S. Akar⁵⁹, P. Albicocco¹⁹, J. Albrecht¹⁰, F. Alessio⁴⁰, M. Alexander⁵³, A. Alfonso Albero³⁸, S. Ali⁴³, G. Alkhazov³¹, P. Alvarez Cartelle⁵⁵, A.A. Alves Jr⁵⁹, S. Amato², S. Amerio²³, Y. Amhis⁷, L. An³, L. Anderlini¹⁸, G. Andreassi⁴¹, M. Andreotti^{17,g}, J.E. Andrews⁶⁰, R.B. Appleby⁵⁶, F. Archilli⁴³, P. d'Argent¹², J. Arnau Romeu⁶, A. Artamonov³⁷, M. Artuso⁶¹, E. Aslanides⁶, M. Atzeni⁴², G. Auriemma²⁶, S. Bachmann¹², J.J. Back⁵⁰, S. Baker⁵⁵, V. Balagura^{7,b}, W. Baldini¹⁷, A. Baranov³⁵, R.J. Barlow⁵⁶, S. Barsuk⁷, W. Barter⁵⁶, F. Baryshnikov³², V. Batozskaya²⁹, V. Battista⁴¹, A. Bay⁴¹, J. Beddow⁵³, F. Bedeschi²⁴, I. Bediaga¹, A. Beiter⁶¹, L.J. Bel⁴³, N. Belyi⁶³, V. Bellee⁴¹, N. Belloli^{21,i}, K. Belous³⁷, I. Belyaev^{32,40}, E. Ben-Haim⁸, G. Bencivenni¹⁹, S. Benson⁴³, S. Beranek⁹, A. Berezhnoy³³, R. Bernet⁴², D. Berninghoff¹², E. Bertholet⁸, A. Bertolin²³, C. Betancourt⁴², F. Betti^{15,40}, M.O. Bettler⁴⁹, M. van Beuzekom⁴³, Ia. Bezshyiko⁴², S. Bifani⁴⁷, P. Billoir⁸, A. Birnkraut¹⁰, A. Bizzeti^{18,u}, M. Bjørn⁵⁷, T. Blake⁵⁰, F. Blanc⁴¹, S. Blusk⁶¹, V. Bocci²⁶, O. Boente Garcia³⁹, T. Boettcher⁵⁸, A. Bondar^{36,w}, N. Bondar³¹, S. Borghi^{56,40}, M. Borisjak³⁵, M. Borsato^{39,40}, F. Bossu⁷, M. Boubdir⁹, T.J.V. Bowcock⁵⁴, E. Bowen⁴², C. Bozzi^{17,40}, S. Braun¹², M. Brodski⁴⁰, J. Brodzicka²⁷, D. Brundu¹⁶, E. Buchanan⁴⁸, C. Burr⁵⁶, A. Bursche¹⁶, J. Buytaert⁴⁰, W. Byczynski⁴⁰, S. Cadeddu¹⁶, H. Cai⁶⁴, R. Calabrese^{17,g}, R. Calladine⁴⁷, M. Calvi^{21,i}, M. Calvo Gomez^{38,m}, A. Camboni^{38,m}, P. Campana¹⁹, D.H. Campora Perez⁴⁰, L. Capriotti⁵⁶, A. Carbone^{15,e}, G. Carboni²⁵, R. Cardinale^{20,h}, A. Cardini¹⁶, P. Carniti^{21,i}, L. Carson⁵², K. Carvalho Akiba², G. Casse⁵⁴, L. Cassina²¹, M. Cattaneo⁴⁰, G. Cavallero^{20,h}, R. Cenci^{24,p}, D. Chamont⁷, M.G. Chapman⁴⁸, M. Charles⁸, Ph. Charpentier⁴⁰, G. Chatzikonstantinidis⁴⁷, M. Chefdeville⁴, S. Chen¹⁶, S.-G. Chitic⁴⁰, V. Chobanova³⁹, M. Chrzaszcz⁴⁰, A. Chubykin³¹, P. Ciambrone¹⁹, X. Cid Vidal³⁹, G. Ciezarek⁴⁰, P.E.L. Clarke⁵², M. Clemencic⁴⁰, H.V. Cliff⁴⁹, J. Closier⁴⁰, V. Coco⁴⁰, J. Cogan⁶, E. Cogneras⁵, V. Cogoni^{16,f}, L. Cojocariu³⁰, P. Collins⁴⁰, T. Colombo⁴⁰, A. Comerma-Montells¹², A. Contu¹⁶, G. Coombs⁴⁰, S. Coquereau³⁸, G. Corti⁴⁰, M. Corvo^{17,g}, C.M. Costa Sobral⁵⁰, B. Couturier⁴⁰, G.A. Cowan⁵², D.C. Craik⁵⁸, A. Crocombe⁵⁰, M. Cruz Torres¹, R. Currie⁵², C. D'Ambrosio⁴⁰, F. Da Cunha Marinho², C.L. Da Silva⁷³, E. Dall'Occo⁴³, J. Dalseno⁴⁸, A. Danilina³², A. Davis³, O. De Aguiar Francisco⁴⁰, K. De Bruyn⁴⁰, S. De Capua⁵⁶, M. De Cian⁴¹, J.M. De Miranda¹, L. De Paula², M. De Serio^{14,d}, P. De Simone¹⁹, C.T. Dean⁵³, D. Decamp⁴, L. Del Buono⁸, B. Delaney⁴⁹, H.-P. Dembinski¹¹, M. Demmer¹⁰, A. Dendek²⁸, D. Derkach³⁵, O. Deschamps⁵, F. Dettori⁵⁴, B. Dey⁶⁵, A. Di Canto⁴⁰, P. Di Nezza¹⁹, S. Didenko⁶⁹, H. Dijkstra⁴⁰, F. Dordei⁴⁰, M. Dorigo⁴⁰, A. Dosil Suárez³⁹, L. Douglas⁵³, A. Dovbnya⁴⁵, K. Dreimanis⁵⁴, L. Dufour⁴³, G. Dujany⁸, P. Durante⁴⁰, J.M. Durham⁷³, D. Dutta⁵⁶, R. Dzhelyadin³⁷, M. Dziewiecki¹², A. Dziurda⁴⁰, A. Dzyuba³¹, S. Easo⁵¹, U. Egede⁵⁵, V. Egorychev³², S. Eidelman^{36,w}, S. Eisenhardt⁵², U. Eitschberger¹⁰, R. Ekelhof¹⁰, L. Eklund⁵³, S. Ely⁶¹, A. Ene³⁰, S. Escher⁹, S. Esen¹², H.M. Evans⁴⁹, T. Evans⁵⁷, A. Falabella¹⁵, N. Farley⁴⁷, S. Farry⁵⁴, D. Fazzini^{21,40,i}, L. Federici²⁵, G. Fernandez³⁸, P. Fernandez Declara⁴⁰, A. Fernandez Prieto³⁹, F. Ferrari¹⁵, L. Ferreira Lopes⁴¹, F. Ferreira Rodrigues², M. Ferro-Luzzi⁴⁰, S. Filippov³⁴, R.A. Fini¹⁴, M. Fiorini^{17,g}, M. Firlej²⁸, C. Fitzpatrick⁴¹, T. Fiutowski²⁸, F. Fleuret^{7,b}, M. Fontana^{16,40}, F. Fontanelli^{20,h}, R. Forty⁴⁰, V. Franco Lima⁵⁴, M. Frank⁴⁰, C. Frei⁴⁰, J. Fu^{22,q}, W. Funk⁴⁰, C. Färber⁴⁰, E. Gabriel⁵², A. Gallas Torreira³⁹, D. Galli^{15,e}, S. Gallorini²³, S. Gambetta⁵², M. Gandelman², P. Gandini²², Y. Gao³, L.M. Garcia Martin⁷¹, B. Garcia Plana³⁹, J. García Pardiñas⁴², J. Garra Tico⁴⁹, L. Garrido³⁸, D. Gascon³⁸, C. Gaspar⁴⁰, L. Gavardi¹⁰, G. Gazzoni⁵, D. Gerick¹², E. Gersabeck⁵⁶, M. Gersabeck⁵⁶, T. Gershon⁵⁰, Ph. Ghez⁴, S. Giani⁴¹, V. Gibson⁴⁹, O.G. Girard⁴¹, L. Giubega³⁰, K. Gizzdov⁵², V.V. Gligorov⁸, D. Golubkov³², A. Golutvin^{55,69}, A. Gomes^{1,a}, I.V. Gorelov³³, C. Gotti^{21,i}, E. Govorkova⁴³, J.P. Grabowski¹²,

- R. Graciani Diaz³⁸, L.A. Granado Cardoso⁴⁰, E. Graug  s³⁸, E. Graverini⁴², G. Graziani¹⁸, A. Grecu³⁰, R. Greim⁴³, P. Griffith¹⁶, L. Grillo⁵⁶, L. Gruber⁴⁰, B.R. Gruberg Cazon⁵⁷, O. Gr  nberg⁶⁷, E. Gushchin³⁴, Yu. Guz^{37,40}, T. Gys⁴⁰, C. G  bel⁶², T. Hadavizadeh⁵⁷, C. Hadjivassiliou⁵, G. Haefeli⁴¹, C. Haen⁴⁰, S.C. Haines⁴⁹, B. Hamilton⁶⁰, X. Han¹², T.H. Hancock⁵⁷, S. Hansmann-Menzemer¹², N. Harnew⁵⁷, S.T. Harnew⁴⁸, C. Hasse⁴⁰, M. Hatch⁴⁰, J. He⁶³, M. Hecker⁵⁵, K. Heinicke¹⁰, A. Heister⁹, K. Hennessy⁵⁴, L. Henry⁷¹, E. van Herwijnen⁴⁰, M. He  ⁶⁷, A. Hicheur², D. Hill⁵⁷, P.H. Hopchev⁴¹, W. Hu⁶⁵, W. Huang⁶³, Z.C. Huard⁵⁹, W. Hulsbergen⁴³, T. Humair⁵⁵, M. Hushchyn³⁵, D. Hutchcroft⁵⁴, P. Ibis¹⁰, M. Idzik²⁸, P. Ilten⁴⁷, K. Ivshin³¹, R. Jacobsson⁴⁰, J. Jalocha⁵⁷, E. Jans⁴³, A. Jawahery⁶⁰, F. Jiang³, M. John⁵⁷, D. Johnson⁴⁰, C.R. Jones⁴⁹, C. Joram⁴⁰, B. Jost⁴⁰, N. Jurik⁵⁷, S. Kandybei⁴⁵, M. Karacson⁴⁰, J.M. Kariuki⁴⁸, S. Karodia⁵³, N. Kazeev³⁵, M. Kecke¹², F. Keizer⁴⁹, M. Kelsey⁶¹, M. Kenzie⁴⁹, T. Ketel⁴⁴, E. Khairullin³⁵, B. Khanji¹², C. Khurewathanakul⁴¹, K.E. Kim⁶¹, T. Kirn⁹, S. Klaver¹⁹, K. Klimaszewski²⁹, T. Klimkovich¹¹, S. Koliiev⁴⁶, M. Kolpin¹², R. Kopecna¹², P. Koppenburg⁴³, S. Kotriakhova³¹, M. Kozeiha⁵, L. Kravchuk³⁴, M. Kreps⁵⁰, F. Kress⁵⁵, P. Krokovny^{36,w}, W. Krupa²⁸, W. Krzemien²⁹, W. Kucewicz^{27,l}, M. Kucharczyk²⁷, V. Kudryavtsev^{36,w}, A.K. Kuonen⁴¹, T. Kvaratskheliya^{32,40}, D. Lacarrere⁴⁰, G. Lafferty⁵⁶, A. Lai¹⁶, G. Lanfranchi¹⁹, C. Langenbruch⁹, T. Latham⁵⁰, C. Lazzeroni⁴⁷, R. Le Gac⁶, A. Leflat^{33,40}, J. Lefran  ois⁷, R. Lef  vre⁵, F. Lemaitre⁴⁰, P. Lenisa¹⁷, O. Leroy⁶, T. Lesiak²⁷, B. Leverington¹², P.-R. Li⁶³, T. Li³, Z. Li⁶¹, X. Liang⁶¹, T. Likhomannenko⁶⁸, R. Lindner⁴⁰, F. Lionetto⁴², V. Lisovskyi⁷, X. Liu³, D. Loh⁵⁰, A. Loi¹⁶, I. Longstaff⁵³, J.H. Lopes², D. Lucchesi^{23,o}, M. Lucio Martinez³⁹, A. Lupato²³, E. Luppi^{17,g}, O. Lupton⁴⁰, A. Lusiani²⁴, X. Lyu⁶³, F. Machefert⁷, F. Maciuc³⁰, V. Macko⁴¹, P. Mackowiak¹⁰, S. Maddrell-Mander⁴⁸, O. Maev^{31,40}, K. Maguire⁵⁶, D. Maisuzenko³¹, M.W. Majewski²⁸, S. Malde⁵⁷, B. Malecki²⁷, A. Malinin⁶⁸, T. Maltsev^{36,w}, G. Manca^{16,f}, G. Mancinelli⁶, D. Marangotto^{22,q}, J. Maratas^{5,v}, J.F. Marchand⁴, U. Marconi¹⁵, C. Marin Benito³⁸, M. Marinangeli⁴¹, P. Marino⁴¹, J. Marks¹², G. Martellotti²⁶, M. Martin⁶, M. Martinelli⁴¹, D. Martinez Santos³⁹, F. Martinez Vidal⁷¹, A. Massafferri¹, R. Matev⁴⁰, A. Mathad⁵⁰, Z. Mathe⁴⁰, C. Matteuzzi²¹, A. Mauri⁴², E. Maurice^{7,b}, B. Maurin⁴¹, A. Mazurov⁴⁷, M. McCann^{55,40}, A. McNab⁵⁶, R. McNulty¹³, J.V. Mead⁵⁴, B. Meadows⁵⁹, C. Meaux⁶, F. Meier¹⁰, N. Meinert⁶⁷, D. Melnychuk²⁹, M. Merk⁴³, A. Merli^{22,q}, E. Michielin²³, D.A. Milanes⁶⁶, E. Millard⁵⁰, M.-N. Minard⁴, L. Minzoni¹⁷, D.S. Mitzel¹², A. Mogini⁸, J. Molina Rodriguez^{1,y}, T. Momb  cher¹⁰, I.A. Monroy⁶⁶, S. Monteil⁵, M. Morandin²³, G. Morello¹⁹, M.J. Morello^{24,t}, O. Morgunova⁶⁸, J. Moron²⁸, A.B. Morris⁶, R. Mountain⁶¹, F. Muheim⁵², M. Mulder⁴³, D. M  ller⁴⁰, J. M  ller¹⁰, K. M  ller⁴², V. M  ller¹⁰, P. Naik⁴⁸, T. Nakada⁴¹, R. Nandakumar⁵¹, A. Nandi⁵⁷, I. Nasteva², M. Needham⁵², N. Neri²², S. Neubert¹², N. Neufeld⁴⁰, M. Neuner¹², T.D. Nguyen⁴¹, C. Nguyen-Mau^{41,n}, S. Nieswand⁹, R. Niet¹⁰, N. Nikitin³³, A. Nogay⁶⁸, D.P. O'Hanlon¹⁵, A. Oblakowska-Mucha²⁸, V. Obraztsov³⁷, S. Ogilvy¹⁹, R. Oldeman^{16,f}, C.J.G. Onderwater⁷², A. Ossowska²⁷, J.M. Otalora Goicochea², P. Owen⁴², A. Oyanguren⁷¹, P.R. Pais⁴¹, A. Palano¹⁴, M. Palutan^{19,40}, G. Panshin⁷⁰, A. Papanestis⁵¹, M. Pappagallo⁵², L.L. Pappalardo^{17,g}, W. Parker⁶⁰, C. Parkes⁵⁶, G. Passaleva^{18,40}, A. Pastore¹⁴, M. Patel⁵⁵, C. Patrignani^{15,e}, A. Pearce⁴⁰, A. Pellegrino⁴³, G. Penso²⁶, M. Pepe Altarelli⁴⁰, S. Perazzini⁴⁰, D. Pereima³², P. Perret⁵, L. Pescatore⁴¹, K. Petridis⁴⁸, A. Petrolini^{20,h}, A. Petrov⁶⁸, M. Petruzzo^{22,q}, B. Pietrzyk⁴, G. Pietrzyk⁴¹, M. Pikies²⁷, D. Pinci²⁶, F. Pisani⁴⁰, A. Pistone^{20,h}, A. Piucci¹², V. Placinta³⁰, S. Playfer⁵², M. Plo Casasus³⁹, F. Polci⁸, M. Poli Lener¹⁹, A. Poluektov⁵⁰, N. Polukhina⁶⁹, I. Polyakov⁶¹, E. Polycarpo², G.J. Pomery⁴⁸, S. Ponce⁴⁰, A. Popov³⁷, D. Popov^{11,40}, S. Poslavskii³⁷, C. Potterat², E. Price⁴⁸, J. Prisciandaro³⁹, C. Prouve⁴⁸, V. Pugatch⁴⁶, A. Puig Navarro⁴², H. Pullen⁵⁷, G. Punzi^{24,p}, W. Qian⁶³, J. Qin⁶³, R. Quagliani⁸, B. Quintana⁵, B. Rachwal²⁸, J.H. Rademacker⁴⁸, M. Rama²⁴, M. Ramos Pernas³⁹, M.S. Rangel², F. Ratnikov^{35,x}, G. Raven⁴⁴, M. Ravonel Salzgeber⁴⁰, M. Reboud⁴, F. Redi⁴¹,

S. Reichert¹⁰, A.C. dos Reis¹, C. Remon Alepuz⁷¹, V. Renaudin⁷, S. Ricciardi⁵¹, S. Richards⁴⁸, K. Rinnert⁵⁴, P. Robbe⁷, A. Robert⁸, A.B. Rodrigues⁴¹, E. Rodrigues⁵⁹, J.A. Rodriguez Lopez⁶⁶, A. Rogozhnikov³⁵, S. Roiser⁴⁰, A. Rollings⁵⁷, V. Romanovskiy³⁷, A. Romero Vidal^{39,40}, M. Rotondo¹⁹, M.S. Rudolph⁶¹, T. Ruf⁴⁰, J. Ruiz Vidal⁷¹, J.J. Saborido Silva³⁹, N. Sagidova³¹, B. Saitta^{16,f}, V. Salustino Guimaraes⁶², C. Sanchez Mayordomo⁷¹, B. Sanmartin Sedes³⁹, R. Santacesaria²⁶, C. Santamarina Rios³⁹, M. Santimaria¹⁹, E. Santovetti^{25,j}, G. Sarpis⁵⁶, A. Sarti^{19,k}, C. Satriano^{26,s}, A. Satta²⁵, D. Savrina^{32,33}, S. Schael⁹, M. Schellenberg¹⁰, M. Schiller⁵³, H. Schindler⁴⁰, M. Schmelling¹¹, T. Schmelzer¹⁰, B. Schmidt⁴⁰, O. Schneider⁴¹, A. Schopper⁴⁰, H.F. Schreiner⁵⁹, M. Schubiger⁴¹, M.H. Schune^{7,40}, R. Schwemmer⁴⁰, B. Sciascia¹⁹, A. Sciubba^{26,k}, A. Semennikov³², E.S. Sepulveda⁸, A. Sergi^{47,40}, N. Serra⁴², J. Serrano⁶, L. Sestini²³, P. Seyfert⁴⁰, M. Shapkin³⁷, Y. Shcheglov^{31,†}, T. Shears⁵⁴, L. Shekhtman^{36,w}, V. Shevchenko⁶⁸, B.G. Siddi¹⁷, R. Silva Coutinho⁴², L. Silva de Oliveira², G. Simi^{23,o}, S. Simone^{14,d}, N. Skidmore¹², T. Skwarnicki⁶¹, I.T. Smith⁵², M. Smith⁵⁵, I. Soares Lavra¹, M.D. Sokoloff⁵⁹, F.J.P. Soler⁵³, B. Souza De Paula², B. Spaan¹⁰, P. Spradlin⁵³, F. Stagni⁴⁰, M. Stahl¹², S. Stahl⁴⁰, P. Stefkova⁴¹, S. Stefkova⁵⁵, O. Steinkamp⁴², S. Stemmle¹², O. Stenyakin³⁷, M. Stepanova³¹, H. Stevens¹⁰, S. Stone⁶¹, B. Storaci⁴², S. Stracka^{24,p}, M.E. Stramaglia⁴¹, M. Straticiuc³⁰, U. Straumann⁴², S. Strokov⁷⁰, J. Sun³, L. Sun⁶⁴, K. Swientek²⁸, V. Syropoulos⁴⁴, T. Szumlak²⁸, M. Szymanski⁶³, S. T'Jampens⁴, Z. Tang³, A. Tayduganov⁶, T. Tekampe¹⁰, G. Tellarini¹⁷, F. Teubert⁴⁰, E. Thomas⁴⁰, J. van Tilburg⁴³, M.J. Tilley⁵⁵, V. Tisserand⁵, M. Tobin⁴¹, S. Tolk⁴⁰, L. Tomassetti^{17,g}, D. Tonelli²⁴, R. Tourinho Jadallah Aoude¹, E. Tournefier⁴, M. Traill⁵³, M.T. Tran⁴¹, M. Tresch⁴², A. Trisovic⁴⁹, A. Tsaregorodtsev⁶, A. Tully⁴⁹, N. Tuning^{43,40}, A. Ukleja²⁹, A. Usachov⁷, A. Ustyuzhanin³⁵, U. Uwer¹², C. Vacca^{16,f}, A. Vagner⁷⁰, V. Vagnoni¹⁵, A. Valassi⁴⁰, S. Valat⁴⁰, G. Valenti¹⁵, R. Vazquez Gomez⁴⁰, P. Vazquez Regueiro³⁹, S. Vecchi¹⁷, M. van Veghel⁴³, J.J. Velthuis⁴⁸, M. Veltri^{18,r}, G. Veneziano⁵⁷, A. Venkateswaran⁶¹, T.A. Verlage⁹, M. Vernet⁵, M. Vesterinen⁵⁷, J.V. Viana Barbosa⁴⁰, D. Vieira⁶³, M. Vieites Diaz³⁹, H. Viemann⁶⁷, X. Vilasis-Cardona^{38,m}, A. Vitkovskiy⁴³, M. Vitti⁴⁹, V. Volkov³³, A. Vollhardt⁴², B. Voneki⁴⁰, A. Vorobyev³¹, V. Vorobyev^{36,w}, C. Vof⁹, J.A. de Vries⁴³, C. Vázquez Sierra⁴³, R. Waldi⁶⁷, J. Walsh²⁴, J. Wang⁶¹, M. Wang³, Y. Wang⁶⁵, Z. Wang⁴², D.R. Ward⁴⁹, H.M. Wark⁵⁴, N.K. Watson⁴⁷, D. Websdale⁵⁵, A. Weiden⁴², C. Weisser⁵⁸, M. Whitehead⁹, J. Wicht⁵⁰, G. Wilkinson⁵⁷, M. Wilkinson⁶¹, M.R.J. Williams⁵⁶, M. Williams⁵⁸, T. Williams⁴⁷, F.F. Wilson^{51,40}, J. Wimberley⁶⁰, M. Winn⁷, J. Wishahi¹⁰, W. Wislicki²⁹, M. Witek²⁷, G. Wormser⁷, S.A. Wotton⁴⁹, K. Wyllie⁴⁰, D. Xiao⁶⁵, Y. Xie⁶⁵, A. Xu³, M. Xu⁶⁵, Q. Xu⁶³, Z. Xu³, Z. Xu⁴, Z. Yang³, Z. Yang⁶⁰, Y. Yao⁶¹, H. Yin⁶⁵, J. Yu⁶⁵, X. Yuan⁶¹, O. Yushchenko³⁷, K.A. Zarebski⁴⁷, M. Zavertyaev^{11,c}, L. Zhang³, Y. Zhang⁷, A. Zhelezov¹², Y. Zheng⁶³, X. Zhu³, V. Zhukov^{9,33}, J.B. Zonneveld⁵², S. Zucchelli¹⁵

¹ Centro Brasileiro de Pesquisas Físicas (CBPF), Rio de Janeiro, Brazil² Universidade Federal do Rio de Janeiro (UFRJ), Rio de Janeiro, Brazil³ Center for High Energy Physics, Tsinghua University, Beijing, China⁴ Univ. Grenoble Alpes, Univ. Savoie Mont Blanc, CNRS, IN2P3-LAPP, Annecy, France⁵ Clermont Université, Université Blaise Pascal, CNRS/IN2P3, LPC, Clermont-Ferrand, France⁶ Aix Marseille Univ, CNRS/IN2P3, CPPM, Marseille, France⁷ LAL, Univ. Paris-Sud, CNRS/IN2P3, Université Paris-Saclay, Orsay, France⁸ LPNHE, Université Pierre et Marie Curie, Université Paris Diderot, CNRS/IN2P3, Paris, France⁹ I. Physikalisches Institut, RWTH Aachen University, Aachen, Germany¹⁰ Fakultät Physik, Technische Universität Dortmund, Dortmund, Germany¹¹ Max-Planck-Institut für Kernphysik (MPIK), Heidelberg, Germany¹² Physikalisches Institut, Ruprecht-Karls-Universität Heidelberg, Heidelberg, Germany

- ¹³ School of Physics, University College Dublin, Dublin, Ireland
¹⁴ Sezione INFN di Bari, Bari, Italy
¹⁵ Sezione INFN di Bologna, Bologna, Italy
¹⁶ Sezione INFN di Cagliari, Cagliari, Italy
¹⁷ Universita e INFN, Ferrara, Ferrara, Italy
¹⁸ Sezione INFN di Firenze, Firenze, Italy
¹⁹ Laboratori Nazionali dell'INFN di Frascati, Frascati, Italy
²⁰ Sezione INFN di Genova, Genova, Italy
²¹ Sezione INFN di Milano Bicocca, Milano, Italy
²² Sezione di Milano, Milano, Italy
²³ Sezione INFN di Padova, Padova, Italy
²⁴ Sezione INFN di Pisa, Pisa, Italy
²⁵ Sezione INFN di Roma Tor Vergata, Roma, Italy
²⁶ Sezione INFN di Roma La Sapienza, Roma, Italy
²⁷ Henryk Niewodniczanski Institute of Nuclear Physics Polish Academy of Sciences, Kraków, Poland
²⁸ AGH - University of Science and Technology, Faculty of Physics and Applied Computer Science, Kraków, Poland
²⁹ National Center for Nuclear Research (NCBJ), Warsaw, Poland
³⁰ Horia Hulubei National Institute of Physics and Nuclear Engineering, Bucharest-Magurele, Romania
³¹ Petersburg Nuclear Physics Institute (PNPI), Gatchina, Russia
³² Institute of Theoretical and Experimental Physics (ITEP), Moscow, Russia
³³ Institute of Nuclear Physics, Moscow State University (SINP MSU), Moscow, Russia
³⁴ Institute for Nuclear Research of the Russian Academy of Sciences (INR RAS), Moscow, Russia
³⁵ Yandex School of Data Analysis, Moscow, Russia
³⁶ Budker Institute of Nuclear Physics (SB RAS), Novosibirsk, Russia
³⁷ Institute for High Energy Physics (IHEP), Protvino, Russia
³⁸ ICCUB, Universitat de Barcelona, Barcelona, Spain
³⁹ Instituto Galego de Física de Altas Enerxías (IGFAE), Universidade de Santiago de Compostela, Santiago de Compostela, Spain
⁴⁰ European Organization for Nuclear Research (CERN), Geneva, Switzerland
⁴¹ Institute of Physics, Ecole Polytechnique Fédérale de Lausanne (EPFL), Lausanne, Switzerland
⁴² Physik-Institut, Universität Zürich, Zürich, Switzerland
⁴³ Nikhef National Institute for Subatomic Physics, Amsterdam, The Netherlands
⁴⁴ Nikhef National Institute for Subatomic Physics and VU University Amsterdam, Amsterdam, The Netherlands
⁴⁵ NSC Kharkiv Institute of Physics and Technology (NSC KIPT), Kharkiv, Ukraine
⁴⁶ Institute for Nuclear Research of the National Academy of Sciences (KINR), Kyiv, Ukraine
⁴⁷ University of Birmingham, Birmingham, United Kingdom
⁴⁸ H.H. Wills Physics Laboratory, University of Bristol, Bristol, United Kingdom
⁴⁹ Cavendish Laboratory, University of Cambridge, Cambridge, United Kingdom
⁵⁰ Department of Physics, University of Warwick, Coventry, United Kingdom
⁵¹ STFC Rutherford Appleton Laboratory, Didcot, United Kingdom
⁵² School of Physics and Astronomy, University of Edinburgh, Edinburgh, United Kingdom
⁵³ School of Physics and Astronomy, University of Glasgow, Glasgow, United Kingdom
⁵⁴ Oliver Lodge Laboratory, University of Liverpool, Liverpool, United Kingdom
⁵⁵ Imperial College London, London, United Kingdom
⁵⁶ School of Physics and Astronomy, University of Manchester, Manchester, United Kingdom
⁵⁷ Department of Physics, University of Oxford, Oxford, United Kingdom
⁵⁸ Massachusetts Institute of Technology, Cambridge, MA, United States
⁵⁹ University of Cincinnati, Cincinnati, OH, United States
⁶⁰ University of Maryland, College Park, MD, United States

- ⁶¹ *Syracuse University, Syracuse, NY, United States*
- ⁶² *Pontifícia Universidade Católica do Rio de Janeiro (PUC-Rio), Rio de Janeiro, Brazil, associated to* ²
- ⁶³ *University of Chinese Academy of Sciences, Beijing, China, associated to* ³
- ⁶⁴ *School of Physics and Technology, Wuhan University, Wuhan, China, associated to* ³
- ⁶⁵ *Institute of Particle Physics, Central China Normal University, Wuhan, Hubei, China, associated to* ³
- ⁶⁶ *Departamento de Fisica, Universidad Nacional de Colombia, Bogota, Colombia, associated to* ⁸
- ⁶⁷ *Institut für Physik, Universität Rostock, Rostock, Germany, associated to* ¹²
- ⁶⁸ *National Research Centre Kurchatov Institute, Moscow, Russia, associated to* ³²
- ⁶⁹ *National University of Science and Technology MISIS, Moscow, Russia, associated to* ³²
- ⁷⁰ *National Research Tomsk Polytechnic University, Tomsk, Russia, associated to* ³²
- ⁷¹ *Instituto de Fisica Corpuscular, Centro Mixto Universidad de Valencia - CSIC, Valencia, Spain, associated to* ³⁸
- ⁷² *Van Swinderen Institute, University of Groningen, Groningen, The Netherlands, associated to* ⁴³
- ⁷³ *Los Alamos National Laboratory (LANL), Los Alamos, United States, associated to* ⁶¹
- ^a *Universidade Federal do Triângulo Mineiro (UFTM), Uberaba-MG, Brazil*
- ^b *Laboratoire Leprince-Ringuet, Palaiseau, France*
- ^c *P.N. Lebedev Physical Institute, Russian Academy of Science (LPI RAS), Moscow, Russia*
- ^d *Università di Bari, Bari, Italy*
- ^e *Università di Bologna, Bologna, Italy*
- ^f *Università di Cagliari, Cagliari, Italy*
- ^g *Università di Ferrara, Ferrara, Italy*
- ^h *Università di Genova, Genova, Italy*
- ⁱ *Università di Milano Bicocca, Milano, Italy*
- ^j *Università di Roma Tor Vergata, Roma, Italy*
- ^k *Università di Roma La Sapienza, Roma, Italy*
- ^l *AGH - University of Science and Technology, Faculty of Computer Science, Electronics and Telecommunications, Kraków, Poland*
- ^m *LIFAELS, La Salle, Universitat Ramon Llull, Barcelona, Spain*
- ⁿ *Hanoi University of Science, Hanoi, Vietnam*
- ^o *Università di Padova, Padova, Italy*
- ^p *Università di Pisa, Pisa, Italy*
- ^q *Università degli Studi di Milano, Milano, Italy*
- ^r *Università di Urbino, Urbino, Italy*
- ^s *Università della Basilicata, Potenza, Italy*
- ^t *Scuola Normale Superiore, Pisa, Italy*
- ^u *Università di Modena e Reggio Emilia, Modena, Italy*
- ^v *Iligan Institute of Technology (IIT), Iligan, Philippines*
- ^w *Novosibirsk State University, Novosibirsk, Russia*
- ^x *National Research University Higher School of Economics, Moscow, Russia*
- ^y *Escuela Agrícola Panamericana, San Antonio de Oriente, Honduras*
- [†] *Deceased*